Photon recycling effect on electroluminescent refrigeration

Kuan-Chen Lee and Shun-Tung Yen

Citation: Journal of Applied Physics **111**, 014511 (2012); doi: 10.1063/1.3676249
View online: http://dx.doi.org/10.1063/1.3676249
View Table of Contents: http://scitation.aip.org/content/aip/journal/jap/111/1?ver=pdfcov
Published by the AIP Publishing

Photon recycling effect on electroluminescent refrigeration

Kuan-Chen Lee and Shun-Tung Yen[a)]
Department of Electronics Engineering and Institute of Electronics, National Chiao Tung University, 1001 Ta-Hsueh Road, Hsinchu, Taiwan

(Received 4 August 2011; accepted 12 December 2011; published online 13 January 2012)

We study electroluminescent refrigeration in an AlGaAs/GaAs double heterostructure by a self-consistent calculation with photon recycling considered. To gain insight, we investigate the influence of the recycling on the carrier density and the current components due to various recombination mechanisms in the device under different bias voltages. The photon recycling is a feedback process, which behaves as an internal source of generating electron-hole pairs in the active region and causes an effective feedback current to compensate the driving current from the external source. Consequently, it reduces the driving current, improves the external quantum efficiency, and loosens the requirement on the photon extraction efficiency for refrigeration. For the device with a 1 μm GaAs active layer operating at 300 K, the minimum required extraction efficiency is less than 20% if the trapped photons are completely recycled and remains a feasible value of 45% if the recycling efficiency is 90%, which is not difficult to achieve. In addition, photon recycling eases the problem of the drastic deterioration of the cooling power and the external efficiency as the extraction efficiency reduces. These results reveal a good possibility of realizing electroluminescent refrigeration in semiconductors. © *2012 American Institute of Physics*. [doi:10.1063/1.3676249]

I. INTRODUCTION

Optical refrigeration in solids has attracted significant interest since the first demonstration of photoluminescent (PL) refrigeration in 1995.[1] To date, it has been shown that an Yb-doped $LiYF_4$ crystal is capable of reducing the temperature down to 155 K with a cooling power of 90 mW.[2] Further reduction of the temperature below 100 K seems difficult to achieve in such a rare-earth doped system. This is because the cooling process becomes inefficient as the thermal energy approaches the energy difference between levels of the ground-state manifold.[3,4] Compared to the rare-earth doped cooler, a semiconductor luminescent cooler has no such limitation and is expected to have the potential of lower operation temperature and higher cooling power density. Additionally, it can be integrated directly with other semiconductor devices. These attractive features have stimulated extensive research in semiconductor PL refrigeration.[5–9] However, experimental demonstration of semiconductor PL cooling has not been realized, mainly due to the harsh requirement of a nearly 100% external quantum efficiency (EQE) for semiconductors with bandgap energies larger than 1 eV.

Recently, semiconductor luminescent refrigeration using an electrical pumping scheme has received growing attention because of its looser requirement on EQE compared with semiconductor PL refrigeration.[10] Several theoretical studies have been carried out to investigate the cooling feasibility and capability of semiconductor electroluminescent (EL) refrigeration.[10–14] Mal'shukov and Chao studied the influence of the Auger recombination on the cooling capability of a GaAs embedded double heterostructure (DH).[11] They showed that a net cooling power density of several W/cm^2 is achievable, even if the Auger recombination coefficient is as high as 4×10^{-29} cm^6/s. Later, Wang *et al.* performed a detailed self-consistent calculation with the consideration of various recombination mechanisms.[12] Their analysis showed an impressive cooling efficiency of 35% for a DH with a *p*-GaAs active layer. Recently, we studied the influence of the current leakage and the active layer thickness on EL refrigeration.[10] We found that the leakage current can be eliminated almost completely by carrier blocking layers. The study gave a limiting cooling power density of 97 W/cm^2 for AlGaAs/GaAs DH at 300 K. However, the aforementioned studies did not take into account the photon recycling effect.[15] In the absence of photon recycling, the extraction efficiency required for cooling would be at least 75%.[10,12] Achieving such a tight requirement is a challenge to the state-of-the-art technology, and the difficulty has been obstructing the realization of semiconductor EL cooling.

It was shown that photon recycling can significantly reduce the extraction efficiency required for semiconductor PL refrigeration from 98% to 5%.[16] However, the photon recycling effect on EL refrigeration has not yet been studied thoroughly. Recently, Heikkilä *et al.* performed a self-consistent calculation and used a semiquantitative model to study the ultimate efficiency of AlGaAs/GaAs DH light-emitting diodes with the consideration of the photon recycling effect.[17,18] Their works mainly focused on a specific case of constant extraction efficiency and optical parasitic loss. It was left open how the photon recycling influences the operation of the EL refrigerator under various external bias voltages through various microscopic electric and optical processes.

In this work, we investigate the photon recycling effect by a self-consistent calculation on the cooling capability,

[a)]Electronic mail: styen@cc.nctu.edu.tw.

the internal and external efficiencies, and the electrical properties of an AlGaAs/GaAs DH EL refrigerator. We find that the photon recycling works as an internal pumping source to supply electron-hole pairs, which mediate as the refrigerant for extraction of internal energy through thermalization and radiative recombination in the active layer. The effect can be modeled as an effective feedback current, which compensates the driving current from the external source. As a consequence, the photon recycling can reduce considerably the driving current for a device biased at a given voltage and, hence, improve the EQE. Additionally, the recycling alleviates the requirement on the extraction efficiency for refrigeration, because it does not dissipate the photon energy, but transforms the photons into the workable potential energy in the form of electron-hole pairs. The minimum required extraction efficiency is less than 20% if the trapped photons were all reincarnated into electron-hole pairs and remains a feasible value of about 45% if the photon recycling efficiency is taken as a more practical value of 90%.

This paper is organized as follows. In Sec. II, we will first explain about the operation principle of the EL refrigerator and then describe the self-consistent method for the calculation of the work. Calculated results together with analysis and discussion will be given in Sec. III. Finally, we draw a conclusion in Sec. IV.

II. THEORETICAL APPROACHES

We consider a *p-i-n* heterojunction structure, whose band diagram is shown in Fig. 1. It was formed, in order, with a 100-nm *p*-$Al_{0.25}Ga_{0.75}As$ cladding layer (with an acceptor concentration $N_a = 10^{18}$ cm^{-3}), a 50-nm $p - Al_{0.4}Ga_{0.6}As$ electron blocking layer (with $N_a = 10^{18}$ cm^{-3}), a 50-nm undoped $Al_{0.25}Ga_{0.75}As$ spacer layer, a 1-μm undoped GaAs active layer, a 50-nm undoped $Al_{0.25}Ga_{0.75}As$ spacer layer, a 50-nm *n*-$Al_{0.4}Ga_{0.6}As$ hole blocking layer (with a donor concentration $N_d = 10^{18}$ cm^{-3}), and a 100-nm *n*-$Al_{0.25}Ga_{0.75}As$ cladding layer (with $N_d = 10^{18}$ cm^{-3}). Figure 1 also shows the quasi-Fermi level profiles, E_{Fc} and E_{Fv}, as well as the energy band profiles, E_c and E_v, of the conduction and the valence bands, respectively, along the growth direction (defined as the axis z) under a forward bias of 1.4 V. These profiles are obtained from the self-consistent calculation to be described. The calculation approach is similar to that in our previous work,[10] except that we consider the photon recycling in the present calculation.

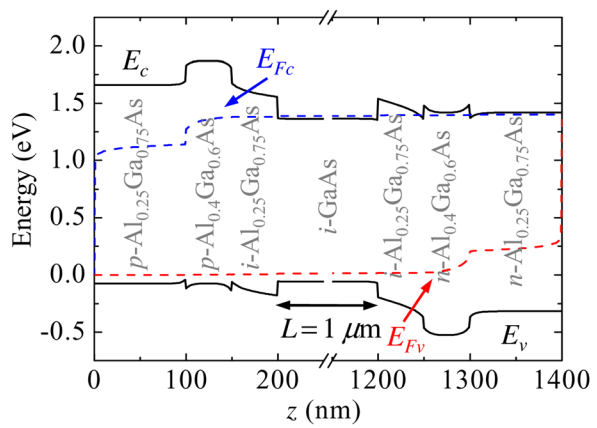

FIG. 1. (Color online) The energy band profiles, E_c and E_v, and the quasi-Fermi level profiles, E_{Fc} and E_{Fv}, of the conduction and the valence bands, respectively, along the growth direction z. The active layer thickness L is 1 μm. The profiles are a result of our self-consistent calculation at a forward bias of 1.4 V.

A. Operation principle of EL refrigerators with photon recycling

Photon recycling is a feedback process. The operation of an EL refrigerator with photon recycling can be figured out with the aid of the diagram in Fig. 2. Electrons and holes injected from the electrodes under a forward bias cause an electric current J in the device. Most of the electrons and holes are intended to be injected into the active region, recombine therein, and then result in a major part of the current, called the injection current J_{inj}. The injection efficiency η_{inj} is defined as the ratio J_{inj}/J. The other small part of the current, called the leakage current J_{leak}, arises from recombinations of electrons and holes residing out of the active region. There are two means of injecting carriers to the active region. One is by external electric injection, as described previously. The other is by internal optical excitation if photons of sufficient energy are present. The generation of electron-hole pairs by optical excitation is modeled as an effective current J_G, while the electric injection results in

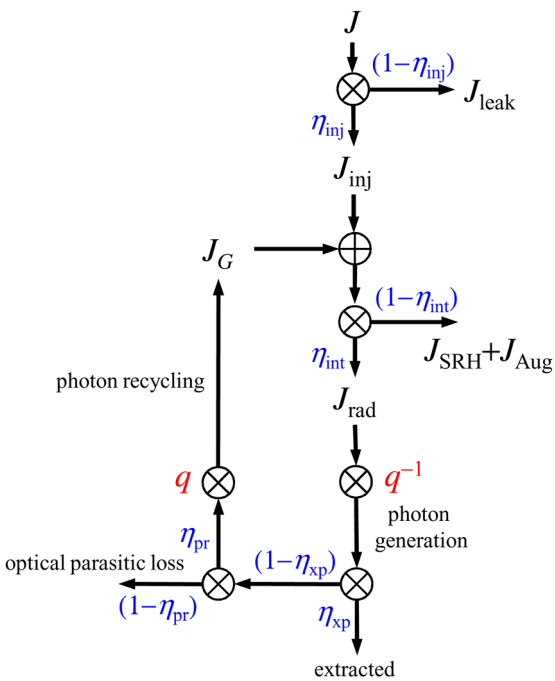

FIG. 2. (Color online) The diagram for illustration of the operation of an electroluminescent refrigerator with photon recycling as a feedback. It indicates the relationships among various currents, including the driving current J, the leakage current J_{leak}, the SRH recombination current J_{SRH}, the Auger recombination current J_{Aug}, the radiative recombination current J_{rad}, and the optical generation current J_G. Symbol $\oplus$ stands for an addition operation which sums its inputs, indicated by inward arrows with the tips pointing at the symbol, and gives its output, indicated by an outward arrow with the tip pointing away from the symbol. Symbols $\otimes$ stand for multiplication operations, which give their outputs, indicated by outward arrows, by multiplying their inputs, indicated by inward arrows, by the factors along with the individual outward arrows.

the injection current J_{inj}. As a result, the sum $J_{inj}+J_G$ accounts for the total effective injection rate of electrons and holes to the active region. In the steady-state condition, the injection rate is balanced by the recombination rate in the active region. Hence,

$$J_{inj}+J_G=J_{rad}+J_{SRH}+J_{Aug}, \tag{1}$$

where J_{rad}, J_{SRH}, and J_{Aug} are the current components due to the radiative, the Shockley-Read-Hall (SRH), and the Auger recombinations, respectively, in the active region. The internal quantum efficiency η_{int} is defined as the ratio $J_{rad}/(J_{rad}+J_{SRH}+J_{Aug})$. Each radiative recombination generates a photon of energy equal to or slightly higher than the bandgap energy of the active region. The resulting photon generation rate is J_{rad}/q, where q is the elementary charge. All the generated photons have a probability of escaping from the device. Such a probability is called the extraction efficiency of photons and denoted by η_{xp}. Hence, the emission rate of photons from the device is $\eta_{xp}J_{rad}/q$. Photons that are trapped within the device are destined for reabsorption. Of the trapped photons, the majority are intended to be recycled with electron-hole pairs created in the active region; the others are reabsorbed parasitically and transformed into thermal energy, leading to the so-called optical parasitic loss. We define the photon recycling efficiency η_{pr} as the percentage of the trapped photons that are eventually recycled. The photon recycling provides one of the two means of injecting carriers to the active region, as has been described. It gives rise to an effective feedback current J_G, which is

$$J_G=\eta_{pr}(1-\eta_{xp})J_{rad}. \tag{2}$$

In conventional optoelectronic devices, the flux of photons emitted from the devices, $\eta_{xp}J_{rad}/q$, is regarded as the output and the current in the devices, J, is the input. The external quantum efficiency η_{ext} is naturally defined as the ratio of the photon flux out of the devices to the carrier flux injected into the devices, i.e., $\eta_{ext}=\eta_{xp}J_{rad}/J$. Equations (1) and (2) combined with the definitions of the various efficiencies allow us to express η_{ext} in terms of the other efficiencies,

$$\eta_{ext}=\frac{\eta_{xp}\eta_{inj}\eta_{int}}{1-\eta_{pr}\eta_{int}(1-\eta_{xp})}. \tag{3}$$

Equation (3) reveals the enhancement of the external efficiency by photon recycling. In the absence of photon recycling ($\eta_{pr}=0$), η_{ext} would be simply the product $\eta_{xp}\eta_{inj}\eta_{int}$. The enhancement factor γ, defined as the ratio of the external efficiency with to without the photon recycling, is thus

$$\gamma=[1-\eta_{pr}\eta_{int}(1-\eta_{xp})]^{-1} \tag{4}$$

if $\eta_{xp}\eta_{inj}\eta_{int}$ is independent of η_{pr}. In practice, Eq. (4) is a good approximation, because $\eta_{xp}\eta_{inj}\eta_{int}$ is generally insensitive to η_{pr}.

The above analysis implies three paths of energy loss that reduces the output. They are the current leakage, the nonradiative electron-hole recombinations in the active region, and the optical parasitic absorption. In the subsequent analysis, we assume that the three loss paths convert the electric energy of carriers or the optical energy of photons into thermal energy in the devices.

Energy can be extracted out of the devices by photon emission and heat transfer. The extracted power is required by energy conservation to equal the input power into the devices at steady state. The input power is JV, where V is the applied voltage. The radiative power P_{rad}, which is the power extracted by photon emission, is the product of the emitted photon flux and the average photon energy $\langle\hbar\omega\rangle$,

$$P_{rad}=\langle\hbar\omega\rangle\eta_{xp}J_{rad}/q. \tag{5}$$

The difference $JV-P_{rad}$ is, therefore, the power extracted out by heat transfer. If the difference is negative, the heat transfer causes a net heat flow into the devices; that is, the devices have the capability of extracting thermal energy from their surroundings to the devices. Accordingly, the cooling power of the devices is defined as

$$P_c=P_{rad}-JV=\eta_cJV, \tag{6}$$

where $\eta_c\equiv P_c/JV$ is known as the cooling efficiency or the coefficient of performance (COP). The notion of EL refrigeration is to set the devices in the cooling mode, where the cooling power $P_c>0$ or $\eta_c>0$. Using Eq. (5) and the definition of $\eta_{ext}=\eta_{xp}J_{rad}/J$, we can rewrite the cooling efficiency as

$$\eta_c=\frac{\eta_{ext}}{\eta_{ext,cr}}-1, \tag{7}$$

where $\eta_{ext,cr}\equiv qV/\langle\hbar\omega\rangle$ is the critical external efficiency for the devices to operate in the cooling mode. From the relation in Eq. (3), we express the critical extraction efficiency as

$$\eta_{xp,cr}=\frac{1-\eta_{pr}\eta_{int}}{\eta_{int}\left(\eta_{inj}/\eta_{ext,cr}-\eta_{pr}\right)}, \tag{8}$$

for $\eta_{inj}/\eta_{ext,cr}>\eta_{pr}$.

B. Self-consistent model

In Subsection II A, we have introduced various terms for describing the operation principle of the EL refrigerator with photon recycling. The operation involves electric processes and optical processes. In this subsection, we present a self-consistent model for quantitative analysis of the device performance through the terms. The model is concerned mainly with the electric conduction in the devices with the electric processes considered in detail. Some of the optical processes, such as photon extraction and photon recycling, are sensitive to the surface, geometry, structure, and material of the devices.[19] We shall not involve ourselves in treating the details of the optical processes in this work, but instead use the extraction efficiency η_{xp} and the photon recycling efficiency η_{pr} as the input parameters.

With η_{xp} and η_{pr} known, the central problem in the calculation turns out to be solving a set of coupled equations for

the profiles E_{Fc}, E_{Fv}, E_c, and E_v, as shown in Fig. 1, since, in the quasi-equilibrium approximation, the profiles can determine the quantities for analyzing the device performance. These quantities include (1) the various concentrations, such as the electron concentration n, the hole concentration p, the ionized donor concentration N_d^+, and the ionized acceptor concentration N_a^-, (2) the various recombination rates, such as the radiative recombination rate $R_{\rm rad}$, the Auger recombination rate $R_{\rm Aug}$, and the SRH recombination rate $R_{\rm SRH}$, (3) the various current components, such as $J_{\rm inj}$, J_G, $J_{\rm rad}$, $J_{\rm Aug}$, $J_{\rm SRH}$, and so forth, and (4) other quantities, such as $\langle\hbar\omega\rangle$, P_c, and the various efficiencies.[10] Refer to Ref. 10 for the relations of these quantities, except J_G, to the profiles E_{Fc}, E_{Fv}, E_c, and E_v.

Since the difference $E_c(z) - E_v(z)$ is the bandgap $E_g(z)$, which is given as an input in the calculation, the bending of the conduction band is the same as that of the valence band. The band bending is described by the electric potential $\Phi(z)$,

$$E_c = E_{c0} - q\Phi, E_v = E_{v0} - q\Phi, \tag{9}$$

where E_{c0} and E_{v0} are the profiles of the conduction and the valence flat bands, respectively. Consequently, we need three equations with proper boundary conditions to solve for the three independent functions $E_{Fc}(z)$, $E_{Fv}(z)$, and $\Phi(z)$. These equations are the one-dimensional Poisson equation,

$$\frac{d}{dz}\epsilon\frac{d}{dz}\Phi = -q(p - n + N_d^+ - N_a^-), \tag{10}$$

and the continuity equations of electrons and holes in the steady state,

$$dJ_n/dz = q(R - G), \tag{11}$$

$$dJ_p/dz = -q(R - G), \tag{12}$$

where ϵ is the electric permittivity, R is the electron-hole recombination rate minus the generation rate due to thermal excitation, G is the electron-hole generation rate due to optical excitation, and J_n and J_p are the drift-diffusion currents of electrons and holes, respectively. The currents J_n and J_p can be expressed by E_{Fc}, E_{Fv}, and Φ,[10] and, as we shall see, all the terms on the right sides of the equations are also determined by E_{Fc}, E_{Fv}, and Φ. Accordingly, Eqs. (10)–(12) can be regarded as a set of coupled differential equations for E_{Fc}, E_{Fv}, and Φ, which will be solved self-consistently.

For the recombination processes, we consider the radiative, the Auger, and the SRH recombinations in the active region and only the SRH recombination outside the active region, as in Ref. 10. The generation rate G is used to account for the photon recycling effect. It is the point of the work. We assume the electron-hole generation associated with photon recycling to occur only in the active region, because the photons are originally created by electron-hole radiative recombinations in the active region, which has a bandgap narrower than the other regions. Furthermore, we assume the optical excitation to generate electron-hole pairs uniformly over the active region. This is justifiable for an active region of thickness no more than 1 μm. As a result, the effective current J_G caused by optical excitation can be simply related to G by

$$J_G = qLG, \tag{13}$$

where L is the thickness of the active region. Comparison between Eqs. (2) and (13) allows expressing

$$G = \frac{1}{qL}\eta_{\rm pr}(1 - \eta_{\rm xp})J_{\rm rad}. \tag{14}$$

We see that G is determined by E_{Fc}, E_{Fv}, and Φ, because so is $J_{\rm rad}$, as has been mentioned.

The boundary conditions for the differential equations (10)–(12) are the same as in Ref. 10. At the interfaces between semiconducting layers, the condition of thermionic emission is used to determine the discontinuity of the quasi-Fermi levels if the band offset is more than twice the thermal energy k_BT, where k_B is the Boltzmann constant and T is the temperature. At the outmost surfaces, we assume an infinite surface recombination velocity, so that the two quasi-Fermi levels merge into the Fermi level of thermal equilibrium. The Fermi levels at the two surfaces are pinned at fixed positions relative to the band edges. Their difference is set at qV, which can be understood as the electric work done on each carrier by the external bias across the device.

III. RESULTS AND DISCUSSION

In this section, we present and analyze the results of the self-consistent calculation for EL refrigeration with photon recycling. In the calculation, the temperature is set at $T = 300$ K. All the material parameters used in this work are the same as in our previous work[10] except for some of those listed in Table I.

In the absence of photon recycling, the performance of the EL refrigerator is sensitive to the photon extraction efficiency, because the photons trapped within the device turn out to be totally absorbed and transformed into thermal energy. The situation is revealed in Fig. 3(a), which shows the curves of the cooling power P_c of the device without photon recycling ($\eta_{\rm pr} = 0$) as a function of the applied voltage V for five values of the extraction efficiency $\eta_{\rm xp} = 0.8$, 0.85, 0.9, 0.95, and 1. The curves exhibit a peak for $\eta_{\rm xp} = 0.9$, 0.95, and 1, but no peak for $\eta_{\rm xp} = 0.8$ and 0.85. As expected, the height of the peak diminishes drastically from 79 to 2 W/cm^2 as $\eta_{\rm xp}$ reduces slightly from unity to 0.9. The voltage at which the curve peaks moves from 1.41 V for $\eta_{\rm xp} = 1$ to 1.28 V for $\eta_{\rm xp} = 0.9$. The cooling power falls rapidly from the peak value to negative as the voltage increases.

TABLE I. Some of the material parameters used in this work. The others can be found from Ref. 10.

Parameters	GaAs	$Al_xGa_{1-x}As$, $x \neq 0$
τ_n (s)	1.3×10^{-6}	10^{-8}
τ_p (s)	10^{-6}	10^{-8}
C_n (cm^{6}s^{-1})	1.9×10^{-31}	–
C_p (cm^{6}s^{-1})	1.2×10^{-30}	–

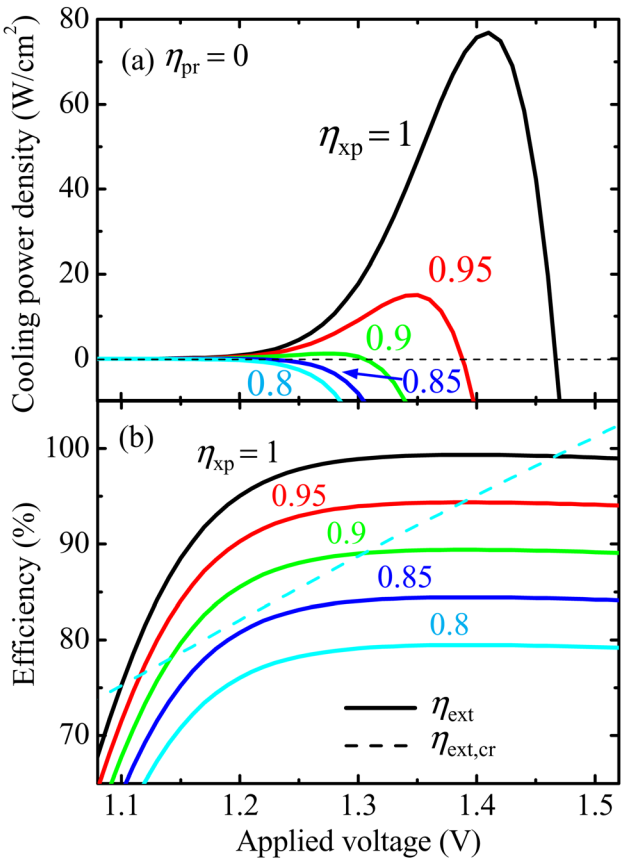

FIG. 3. (Color online) (a) The cooling power density P_c and (b) the external efficiency η_{ext} and the critical external efficiency $\eta_{ext,cr}$ as functions of the applied voltage V for the extraction efficiency $\eta_{xp} = 0.8$, 0.85, 0.9, 0.95, and 1. The photon recycling efficiency is set at $\eta_{pr} = 0$. The dashed lines of $\eta_{ext,cr}$ for the different values of η_{xp} are overlapping.

These behaviors can be understood from Eqs. (6) and (7) with the help of the relationships between the curves of the corresponding external efficiencies η_{ext} and the critical external efficiencies $\eta_{ext,cr}$ shown in Fig. 3(b). The curves of $\eta_{ext,cr}$ for the different η_{xp} values merge into a single line, since $\eta_{ext,cr} \equiv qV/\langle\hbar\omega\rangle$ is nearly proportional to V and independent of η_{xp}. The curves of η_{ext} for the different η_{xp} values behave similarly and separate almost equidistantly from their neighbors. As V increases, the η_{ext} value increases and then almost reaches saturation at a level $\eta_{ext} \approx \eta_{xp}$, with a slight decline in the high-voltage region. These features can be explained by the simple relation $\eta_{ext} = \eta_{xp}\eta_{inj}\eta_{int}$ for $\eta_{pr} = 0$, where the injection efficiency η_{inj} is almost unity for the device containing current blocking layers.[10] Therefore, for $\eta_{xp} = 1$, the variation of η_{ext} with V simply follows the variation of the internal efficiency η_{int}. The curve of η_{ext} for $\eta_{xp} < 1$ is just the curve for $\eta_{xp} = 1$ scaled by the factor η_{xp}. The internal efficiency η_{int} is low at low V, because the SRH recombination is important when the carrier concentration is low. As V increases, the carrier concentration in the active region increases and the radiative recombination becomes increasingly more important than the SRH recombination, leading to the increase in η_{int}. The increase continues until η_{int} reaches a value of nearly unity. The slight decrease of η_{ext} or η_{int} in the high-voltage region is caused by the growing importance of the Auger recombination. From Fig. 3(b), we see that there exist operation regions of refrigeration for $\eta_{xp} = 0.9$, 0.95, and 1, but no operation region for $\eta_{xp} = 0.8$ and 0.85, where the operation region of refrigeration is a range of voltage in which the device operates in the cooling mode ($\eta_c > 0$ or $\eta_{ext} > \eta_{ext,cr}$). This explains the feature in Fig. 3(a) that only the three curves for $\eta_{xp} = 0.9$, 0.95, and 1 exhibit a peak of positive P_c. According to Eq. (7), we can estimate from Fig. 3(b) the voltages at which the η_c-V curves peak for $\eta_{xp} = 0.9$, 0.95, and 1. These voltages are about 1.2 V because, at the voltage, the tangents to the curves of η_{ext}-V are parallel to the line of $\eta_{ext,cr}$. Since the cooling power $P_c = \eta_c JV$, the P_c-V curves peak at voltages higher than the η_c-V curves for $\eta_{xp} = 0.9$, 0.95, and 1. The peaks of P_c-V curves occur at voltages near the critical voltages. The critical voltage is the point where $P_c = 0$ ($\eta_c = 0$), that is, the point where the η_{ext}-V curve crosses the $\eta_{ext,cr}$-V line. This explains that a slight increase of V causes the drastic reduction of P_c from the peak value and may turn the operation of the device from the cooling mode to the heating mode.

In reality, most of the trapped photons are reincarnated into electron-hole pairs rather than into the thermal energy in the high-quality GaAs/AlGaAs heterostructure. The photon recycling, which is neglected above, alleviates considerably the requirement of extraction efficiency for EL refrigeration. To demonstrate the photon-recycling effect, we consider another extreme case by setting $\eta_{pr} = 1$ in the calculation. That is, we assume that the trapped photons are all recycled to generate electron-hole pairs in the active region. The resulting cooling power P_c as a function of V is shown in Fig. 4(a) for five values of the extraction efficiency $\eta_{xp} = 0.2$, 0.4, 0.6, 0.8, and 1. All the curves in the figure behave as an asymmetrical peak of positive P_c, even for the low extraction efficiency of 0.2. The height of the peak now diminishes gently as η_{xp} reduces. These peaks occur almost at the same voltage ($V = 1.41$ V), except for $\eta_{xp} = 0.2$, for which the curve peaks at 1.39 V. Similarly, these behaviors can be understood from Eqs. (6) and (7) and the relationships between the corresponding η_{ext} and $\eta_{ext,cr}$ shown in Fig. 4(b). Compared with those in Fig. 3(b), the external efficiencies η_{ext} in Fig. 4(b) still vary with V in the manner that they first rise, reach a maximum, and then slightly decline. The difference is that η_{ext} is now much less sensitive to η_{xp}, especially in the voltage range where the internal efficiency η_{int} is near unity. In the voltage range between 1.3 V and 1.5 V, where η_{int} is close to unity [Fig. 4(c)], the external efficiency η_{ext} can be approximated by

$$\eta_{ext} \approx \eta_{inj}\left[1 - \frac{1}{\eta_{xp}}(1 - \eta_{int})\right]. \quad (15)$$

Equation (15) explains that, as $1 - \eta_{int}$ is small, the η_{ext} is insensitive to η_{xp} and has a value close to η_{inj}, which is nearly unity, as shown in Fig. 4(c).

In principle, the variation of η_{ext} basically follows the variation of η_{int} modified by photon recycling. This is because the only important loss is the nonradiative recombination in the active region when we set $\eta_{pr} = 1$ and $\eta_{inj} \approx 1$.

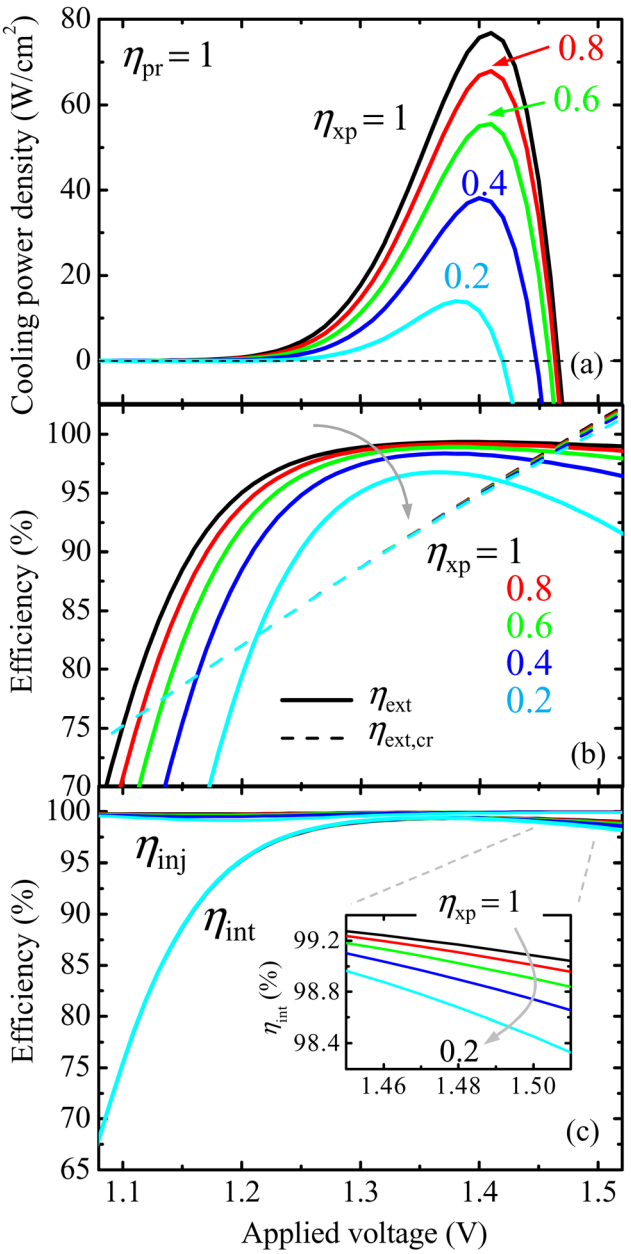

FIG. 4. (Color online) (a) The cooling power density P_c, (b) the external efficiency η_{ext} and the critical external efficiency $\eta_{ext,cr}$, and (c) the injection efficiency η_{inj} and the internal efficiency η_{int} as functions of the applied voltage V for $\eta_{xp} = 0.2$, 0.4, 0.6, 0.8, and 1. The photon recycling efficiency is set at $\eta_{pr} = 1$. The inset of (c) is a magnification of the η_{int} curves in the high-voltage region.

For $\eta_{xp} = 1$, all the generated photons are emitted out of the device and there is no photon recycling, regardless of the value of η_{pr}, as can also be seen from Eq. (3). The photon recycling effect becomes manifest when η_{xp} deviates from unity. It causes an effective feedback current J_G and boosts the carrier concentration in the active region. The increasing carrier concentration degrades η_{int} and, hence, η_{ext} in the high-voltage region. This effect is particularly important for a low η_{xp} [see Fig. 4(b) and the inset in Fig. 4(c)]. The lines of $\eta_{ext,cr}$ in Fig. 4(b) do not merge as completely as those in Fig. 3(b). This is a consequence of the photon-recycling effect, which causes a higher average photon energy $\langle \hbar\omega \rangle$ and, hence, a lower $\eta_{ext,cr}$ for a lower η_{xp}, due to a higher carrier concentration.

The condition that $P_c = 0$ occurs at critical voltages of about 1.47 V for $\eta_{xp} = 0.4$, 0.6, 0.8, and 1. The voltages are close to each other because of the crowding of the η_{ext}-V curves in the high-voltage region, which cross the $\eta_{ext,cr}$-V curves in the vicinity of 1.47 V. This implies that the η_{ext}-V curves peak almost at the same voltage.

Under the condition that $\eta_{pr} = 1$ and $\eta_{inj} \approx 1$, the critical extraction efficiency $\eta_{xp,cr}$ for the device to operate in the cooling mode can be written as

$$\eta_{xp,cr} \approx \frac{(1/\eta_{int}) - 1}{(1/\eta_{ext,cr}) - 1}. \tag{16}$$

The above expression implies that the $\eta_{xp,cr}$ can be very small when η_{int} approaches unity, while $\eta_{ext,cr}$ does not. An EL refrigerator having a very low η_{xp} could operate in the cooling mode if there were no optical parasitic loss ($\eta_{pr} = 1$) and no current leakage ($\eta_{inj} = 1$).

We now know that the internal efficiency η_{int} is an important factor in determining η_{ext} and, hence, to the performance of the device. It is influenced by photon recycling through the feedback generation of electron-hole pairs in the active region. To gain insight into the effect, we set $\eta_{pr} = 1$ and investigate the average carrier density in the active region and the various current components (J_{rad}, J_{SRH}, J_{Aug}, J_{inj}, and J_G) as functions of η_{xp} when the device is biased at $V = 1.2$ V and 1.4 V (Fig. 5). As shown in Fig. 5(a), the average carrier density is low ($\approx 3 \times 10^{16}$ cm^{-3}) and nearly independent of η_{xp} for the device biased at 1.2 V, but is more than 5×10^{17} cm^{-3} and increases as η_{xp} reduces for the device biased at 1.4 V. This difference arises from the difference in the electric potential energy of the electrons (holes) in the active region relative to that in the n-type (p-type) cladding layer, from which the electrons (holes) are injected. When the device is biased at a low voltage, such as $V = 1.2$ V, the electric potential energy of the electrons (holes) is higher in the active region than in the n-type (p-type) cladding layer. This drop in electric potential energy causes the excess carriers, due to optical generation, to leak out of the active region, leading to an effective current J_G opposite the injection current J_{inj}. Consequently, accumulation of carriers in the active region is negligible, and the carrier density is basically independent of the photon recycling (and, hence, η_{xp}). The drop in electric potential energy diminishes as the bias increases and, eventually, the situation reverses. At $V = 1.4$ V, the electric potential energy of the electrons (holes) is lower in the active region than in the n-type (p-type) cladding layer. The potential profile now forms a potential well for the carriers and prohibits most of the excess carriers in the active region from leaking out. As a result, the optically generated carriers are mostly accumulated within the active region, recombined therein, and contribute an additional current, known as J_G. The carrier accumulation depends on the photon recycling and becomes particularly important for low η_{xp}, as shown in Fig. 5(a).

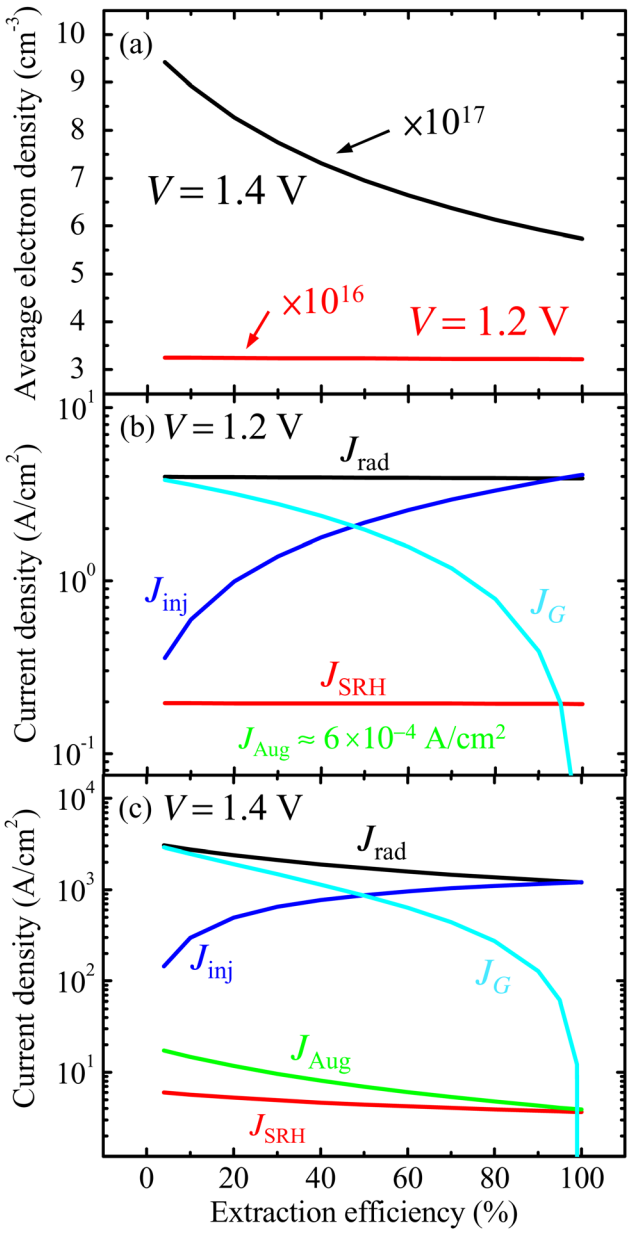

FIG. 5. (Color online) (a) The average electron density in the active layer as a function of the extraction efficiency η_{xp} for the applied voltages $V = 1.2$ and 1.4 V. The current density components J_{rad}, J_{SRH}, J_{Aug}, J_{inj}, and J_G as functions of the extraction efficiency η_{xp} for (b) $V = 1.2$ V and (c) $V = 1.4$ V. The photon recycling efficiency is set at $\eta_{pr} = 1$.

For the device biased at $V = 1.2$ V, the current components J_{rad}, J_{SRH}, and J_{Aug} are also nearly independent of η_{xp}, as shown in Fig. 5(b), because they depend simply on the carrier density in the active region. At such a not-so-low voltage, the current J_{rad} due to radiative recombination predominates overwhelmingly over the other two ($J_{rad} \approx 4$ A/cm^2, $J_{SRH} \approx 0.2$ A/cm^2, $J_{Aug} \approx 6\times 10^{-4}$ A/cm^2), leading to the internal efficiency of 95% shown in Fig. 4(c). The Auger recombination is negligibly small because of the low carrier density. In contrast, the feedback current J_G and the injection current J_{inj} depend strongly on the photon recycling. The former increases almost linearly with $1 - \eta_{xp}$ [Eq. (2)], while the latter decreases almost linearly with $1 - \eta_{xp}$ according to the condition of Eq. (1) that J_G compensates J_{inj} for the total generation rate of carriers in the active region to balance the total recombination rate ($J_{rad} + J_{SRH} + J_{Aug}$), which is nearly independent of η_{xp}. The injection current J_{inj} is much smaller than J_G and J_{rad} for low η_{xp}. Namely, the photon recycling reduces the driving current J, which approximately equals J_{inj} and, hence, enhances the external efficiency η_{ext}. The enhancement factor can be as high as $\gamma = 4.2$ for $\eta_{xp} = 0.2$, according to Eq. (4).

For the device biased at $V = 1.4$ V, the current components J_{rad}, J_{SRH}, and J_{Aug} increase as η_{xp} reduces, in accordance with the variation of the carrier density in the active region. As η_{xp} reduces from 100% to 4%, J_{rad}, J_{SRH}, and J_{Aug} increase from 1200, 4, and 4 A/cm^2 to 3100, 6, and 20 A/cm^2, respectively. Accordingly, the internal efficiency η_{int} changes slightly from 99.34% to 99.17%. The Auger recombination now exceeds the SRH recombination because of the high carrier density, while the radiative recombination remains predominant over the other two. As has been described, the extremely high η_{int} enhances the benefit from the photon recycling. It not only improves the value of η_{ext}, but also eases the deterioration of the device performance due to the reduction in η_{xp}. The external efficiency η_{ext} decreases from 99% to 96% as η_{xp} reduces from 1 to 0.2 for $V = 1.4$ V, as shown in Fig. 4(b), but from 95% to 79% for $V = 1.2$ V, where $\eta_{int} = 95\%$. The high η_{int} of more than 99% keeps the device in the cooling mode, even when the η_{xp} is reduced to 0.2 (Fig. 4).

We have demonstrated the photon recycling effect by setting a complete recycling ($\eta_{pr} = 1$) and comparing the calculated results to those with a null recycling ($\eta_{pr} = 0$). In fact, it is impossible for a device to have a complete photon recycling. A fraction $(1 - \eta_{xp})(1 - \eta_{pr})$ of the photons generated by radiative recombination turn out to be absorbed and transformed into thermal energy. For the device to operate in the cooling mode, parasitic loss of each photon must be covered by emission of a large number of photons, because emission of a photon reduces an amount of internal energy $\langle \hbar\omega \rangle - qV$ in average in the device, which is much smaller than the internal energy generated by parasitic absorption of a photon, qV. As a result, the parasitic absorption is a fatal factor to EL refrigeration and the device performance is expected to be drastically degraded with increasing the factor $(1 - \eta_{xp})(1 - \eta_{pr})$. To manifest the effect of the parasitic absorption, we show in Figs. 6(a) and 6(b) the external efficiency η_{ext} and the enhancement factor γ, respectively, as functions of η_{pr} for $\eta_{xp} = 0.2$, 0.5, and 0.8. The curves are obtained from Eqs. (3) and (4) with $\eta_{inj} = 1$ and $\eta_{int} = 0.99$, corresponding to the applied voltage ranging approximately between 1.3 and 1.45 V [see Fig. 4(b)]. As expected, η_{ext} has a high value predictable from Eq. (15) at $\eta_{pr} = 1$ and then decreases as η_{pr} reduces. The decrease of η_{ext} is more notable for lower η_{xp}, particularly in the region of high η_{pr}. Only in the high η_{pr} region can η_{ext} remain sufficiently high for EL refrigeration. For example, if the device with a high η_{pr} is biased at 1.4 V such that the cooling power reaches approximately at the peak value [Fig. 4(a)], η_{ext} has to exceed the critical value of $\eta_{ext,cr} = 0.95$, indicated by the dashed line in Fig. 6(a) for EL refrigeration. Correspondingly, η_{pr} has to be above 0.85, 0.96, and 0.99 for $\eta_{xp} = 0.8$,

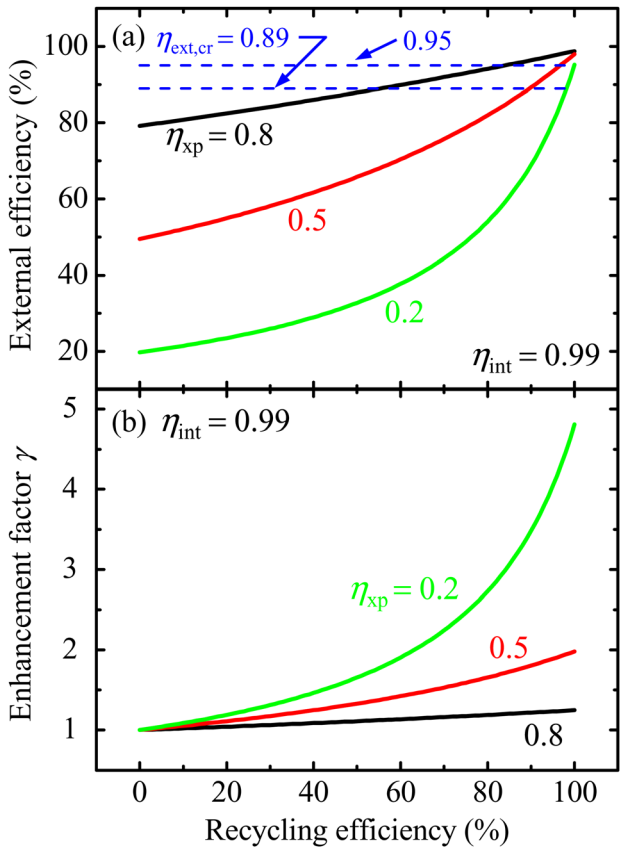

FIG. 6. (Color online) (a) The external efficiency η_{ext} and (b) the enhancement factor γ as functions of the photon recycling efficiency η_{pr} for the extraction efficiency $\eta_{xp} = 0.2$, 0.5, and 0.8. The data are obtained from Eqs. (3) and (4), with the internal efficiency set at $\eta_{int} = 0.99$ and the injection efficiency set at $\eta_{inj} = 1$. The two horizontal dashed lines in (a) denote the critical external efficiencies of $\eta_{ext,cr} = 0.89$ and 0.95, which correspond to the applied voltages of $V = 1.3$ and 1.4 V, respectively.

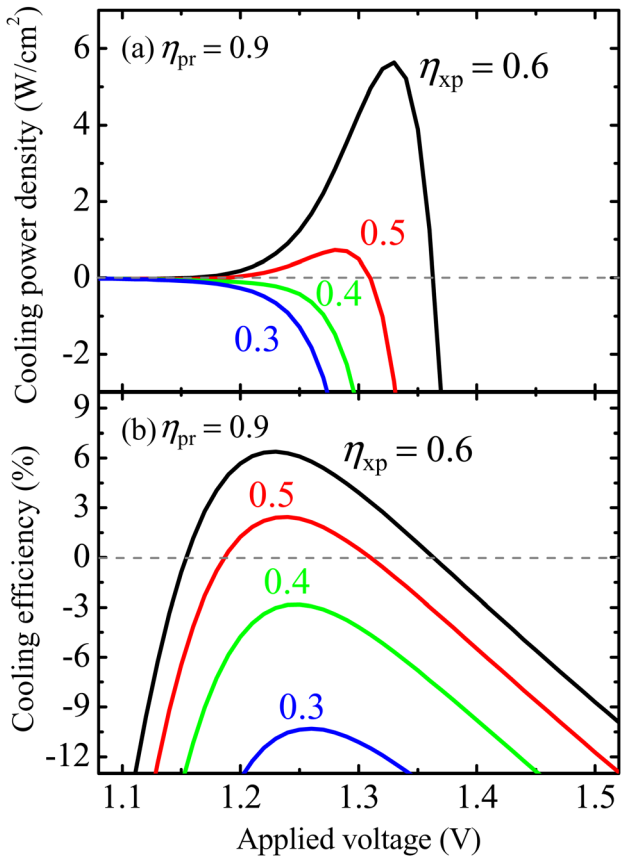

FIG. 7. (Color online) (a) The cooling power density P_c and (b) the cooling efficiency η_c as functions of the applied voltage V for the extraction efficiency $\eta_{xp} = 0.3$, 0.4, 0.5, and 0.6. The recycling efficiency is set at $\eta_{pr} = 0.9$.

0.5, and 0.2, respectively. The tight tolerance can be loosened at the price of the cooling power. If the device is now biased at 1.3 V, the critical external efficiency $\eta_{ext,cr}$ reduces to 0.89, accompanied by a significant reduction in cooling power (Fig. 4). The lower bound of the η_{pr} region for EL refrigeration now extends to 0.55, 0.88, and 0.97 for $\eta_{xp} = 0.8$, 0.5, and 0.2, respectively.

The behavior of the enhancement factor γ in Fig. 6(b) can be understood from the fact that the γ curves can be obtained simply from the η_{ext} curves in Fig. 6(a) normalized by the values of η_{ext} at $\eta_{pr} = 0$ according to the definition of γ. As expected, photon recycling plays a more profound role in improving the performance of the device with a lower η_{xp}.

The quality of the materials making up the device is also important for achieving refrigeration. It is concerned with the nonradiative recombination rate and the optical parasitic absorption and, hence, directly influences η_{int} and η_{pr}. If the material quality is not as high as in the study and gives $\eta_{int} < \eta_{ext,cr}$, it is impossible for the device to operate in the cooling mode as a result of the inequality $\eta_{ext} < \eta_{int}$, regardless of the values of the other efficiencies. In this case, the corresponding η_{ext} curves will lie totally below the dashed line of $\eta_{ext,cr}$, as in Fig. 6(a).

Finally, we show in Figs. 7(a) and 7(b) the cooling power P_c and the cooling efficiency η_c, respectively, as functions of applied voltage V for cases more practical than the previous cases of Figs. 3 and 4. For the device containing a 1-μm active layer, η_{xp} is at most 60%.[20] We therefore consider $\eta_{xp} = 0.3$, 0.4, 0.5, and 0.6 and set $\eta_{pr} = 0.9$, which is not difficult to reach for high-quality GaAs material. The resulting P_c-V relationship changes with η_{xp} to a degree milder than for $\eta_{pr} = 0$ [Fig. 3(a)] but more severe than for $\eta_{pr} = 1$ [Fig. 4(a)]. The peak cooling power is now 5.6 W/cm^2 at $V = 1.33$ V for $\eta_{xp} = 0.6$, which is only 10% of the corresponding value when $\eta_{pr} = 1$. At the voltage of 1.33 V, the cooling efficiency η_c is small (2%) for $\eta_{xp} = 0.6$ and falls negative as η_{xp} reduces to 0.5, associated with the severe degradation of P_c from 5.6 to -3 W/cm^2. The situation can be cured by biasing the device at a lower voltage for an improved η_c. For example, at $V = 1.24$ V, η_c is 6.4% for $\eta_{xp} = 0.6$ and remains positive (about 2%) for $\eta_{xp} = 0.5$. The device can operate in the cooling mode for $\eta_{xp} > 0.45$. However, the cooling power is sacrificed. It is now only 0.9 W/cm^2 for $\eta_{xp} = 0.6$ and 0.3 W/cm^2 for $\eta_{xp} = 0.5$.

IV. CONCLUSION

We have investigated the photon recycling effect on electroluminescent refrigeration by self-consistent calculation. The photon recycling can alleviate considerably the requirement for refrigeration. It behaves as an additional means of generating carriers, reduces the driving current in the device, and improves the external efficiency. A photon

recycling efficiency of 90% can improve the external efficiency by a factor of 4 for the device with an extraction efficiency of $\eta_{xp} = 20\%$ and an internal efficiency of $\eta_{int} = 99\%$. Consequently, the device can operate in the cooling mode, even if the extraction efficiency is not high. For example, for a device that has a 1-μm GaAs active layer and operates at $T = 300$ K, the condition of $\eta_{xp} = 60\%$ and $\eta_{pr} = 90\%$ gives a peak cooling power of 5.6 W/cm^2 at $V = 1.33$ V associated with a low cooling efficiency of 2% and a tight tolerance to the extraction efficiency. The tolerance can be loosened at the cost of cooling power. The device can operate in the cooling mode for $\eta_{xp} > 45\%$ when biased at 1.24 V. The results reveal a good possibility of experimentally achieving electroluminescent refrigeration in semiconductors.

ACKNOWLEDGMENTS

This work was supported by National Science Council of the Republic of China under Contract No. 99-2120 -M-009-009 -.

[1]R. I. Epstein, M. I. Buchwald, B. C. Edwards, T. R. Gosnell, and C. E. Mungan, Nature (London) **377**, 500 (1995).
[2]D. V. Seletskiy, S. D. Melgaard, S. Bigotta, A. D. Lieto, M. Tonelli, and M. Sheik-Bahae, Nat. Photonics **4**, 161 (2010).
[3]M. Sheik-Bahae and R. I. Epstein, Nat. Photonics **1**, 693 (2007).
[4]M. Sheik-Bahae and R. I. Epstein, Laser Photonics Rev. **3**, 67 (2009).
[5]M. Sheik-Bahae and R. I. Epstein, Phys. Rev. Lett. **92**, 247403 (2004).
[6]D. Huang, T. Apostolova, P. M. Alsing, and D. A. Cardimona, Phys. Rev. B **70**, 033203 (2004).
[7]G. Rupper, N. H. Kwong, and R. Binder, Phys. Rev. B **76**, 245203 (2007).
[8]G. Rupper, N. H. Kwong, R. Binder, C.-Y. Li, and M. Sheik-Bahae, J. Appl. Phys. **108**, 113118 (2010).
[9]C. Wang, M. P. Hasselbeck, C.-Y. Li, and M. Sheik-Bahae, Proc. SPIE **7614**, 76140B (2010).
[10]S.-T. Yen and K.-C. Lee, J. Appl. Phys. **107**, 054513 (2010).
[11]A. G. Mal'shukov and K. A. Chao, Phys. Rev. Lett. **86**, 5570 (2001).
[12]J.-B. Wang, D. Ding, S.-Q. Yu, S. R. Johnson, and Y.-H. Zhang, in *Conference on Lasers and Electro-Optics/Quantum Electronics and Laser Science and Photonic Applications Systems Technologies*, Technical Digest (CD) (Optical Society of America, Washington, DC, 2005), paper QThI7.
[13]S.-Q. Yu, J.-B. Wang, D. Ding, S. R. Johnson, D. Vasileska, and Y.-H. Zhang, Solid-State Electron. **51**, 1387 (2007).
[14]J. Oksanen and J. Tulkki, J. Appl. Phys. **107**, 093106 (2010).
[15]I. Schnitzer, E. Yablonovitch, C. Caneau, and T. J. Gmitter, Appl. Phys. Lett. **62**, 131 (1993).
[16]J.-B. Wang, S. R. Johnson, D. Ding, S.-Q. Yu, and Y.-H. Zhang, J. Appl. Phys. **100**, 043502 (2006).
[17]O. Heikkilä, J. Oksanen, and J. Tulkki, J. Appl. Phys. **105**, 093119 (2009).
[18]O. Heikkilä, J. Oksanen, and J. Tulkki, J. Appl. Phys. **107**, 033105 (2010).
[19]R. Windisch, C. Rooman, B. Dutta, A. Knobloch, G. Borghs, G. H. Döhler, and P. Heremans, IEEE J. Sel. Top. Quantum Electron. **8**, 248 (2002).
[20]P. Asbeck, J. Appl. Phys. **48**, 820 (1977).